American Mineralogist, Volume 76, pages 74–82, 1991

The metamictization of zircon: Radiation dose-dependent structural characteristics

JAMES A. WOODHEAD
Department of Geology, Occidental College, Los Angeles, California 90041, U.S.A.
GEORGE R. ROSSMAN, LEON T. SILVER
Division of Geological and Planetary Sciences, California Institute of Technology, Pasadena, California 91125, U.S.A.

ABSTRACT

A suite of gem zircon samples from Sri Lanka has been studied using infrared (IR) spectroscopy, X-ray diffraction, and chemical analysis. The degree of metamictization of the zircon, as indicated by unit-cell parameters, increases systematically with U-Th content up to the point of total metamictization. The appearance of IR spectra also varies as a function of metamictization; band widths increase and intensities decrease with increasing U-Th contents. Persistence of bands related to Si-O bonds and disappearance of bands related to Zr-O bonds indicates that the structure of metamict zircon consists of distorted and disoriented isolated silica tetrahedra with few if any undisplaced Zr cations. All spectroscopic indicators of crystalline order show that total metamictization is reached at an accumulated radiation dosage of $\sim 4.5 \times 10^{15}$ alpha decay events per mg. Hydrous components enter the structure only after total metamictization, but the amounts are not correlated with U-Th content. In all cases OH was the only hydrous species detected.

INTRODUCTION

Metamictization of natural zircon results from accumulated radiation damage to the crystal structure caused by radioactive decay of trace amounts of U and Th substituting for Zr. The damage is generally considered to be the result of recoiling nuclei produced in the α-emission process (Holland and Gottfried, 1955; Headley et al., 1982), although others have attributed it to spontaneous fission of ^{238}U (Yada et al., 1981, 1987). Metamictization is characterized by marked changes in physical properties, including significant decreases in density, refractive index, and birefringence (Holland and Gottfried, 1955). Changes in the susceptibility of the contained U-Th-radiogenic Pb isotope system to chemical disturbance, important in geochronology, parallel the increases in radiation damage (Silver and Deutsch, 1963; Silver, 1964; Pidgeon et al., 1973).

Details of the transitional and final structures of zircon undergoing metamictization are important to the understanding of the process. The structure of crystalline zircon consists of isolated $[SiO_4]^{4-}$ tetrahedra with strong internal Si-O bonds. The tetrahedra are joined by weaker M-O bonds involving Zr^{4+} cations (and any species substituting for Zr) in eightfold coordination (Robinson et al., 1971; Dawson et al., 1971). The structure of metamict zircon has been the subject of debate. Hypothesized structures for metamict zircon include slightly misoriented zircon crystallites (Bursill and McLaren, 1966) and mixtures of crystalline SiO_2 and ZrO_2 (Pellas, 1965; Wasilewski et al., 1973). These proposals seem unlikely in view of recent X-ray spectroscopic studies (Nakai et al., 1987; Sugiyama and Waseda, 1989; Farges and Calas, 1991). Other proposals more consistent with these recent studies include mixed crystalline and amorphous domains (Sommerauer, 1976) and $ZrSiO_4$ glass (Holland and Gottfried, 1955; Vance, 1975; Yada et al., 1981; Headley et al., 1982). The difference among models for the structure of metamict zircon was the initial impetus for the present study because appreciable fractions of any crystalline phases in metamict samples should be evident in their IR spectra.

IR spectra may also reveal the effects of metamictization at the Si-O and Zr-O bond level because the various IR-absorption bands depend on different segments of the zircon structure. To a first approximation the IR spectrum of zircon is made up of internal modes involving bending and stretching of Si-O bonds in discrete tetrahedral $[SiO_4]^{4-}$ anions and external modes involving translation and rotation of nearly rigid tetrahedra in relation to the Zr cations. Because these bands are well separated, it is possible to follow them independently as metamictization progresses.

Of particular importance to isotope geochronology is the stability of U, Th, and their daughter products in metamict zircon. Zircon is known to be subject to annealing with concomitant disturbance of the isotopic system. H_2O is thought to have a strong effect on metamictization and annealing of zircon but there is little agreement on the nature of that effect. Frondel and Collette (1957) found that H_2O lowers the temperature and increases the rate of recrystallization of metamict zircon in annealing experiments. Pavlovic and Krstanovic (1965) found that H_2O hinders the metamictization process. Pidgeon et al. (1966, 1973) found that in hydrothermal experiments, distilled H_2O had little effect on the rate of recrystalliza-

0003–004X/91/0102–0074$02.00

tion of metamict zircon whereas dilute NaCl solutions had a dramatic effect. More recently Caruba et al. (1985) have synthesized hydroxylated zircon, and after comparing their synthetic products to natural samples, conclude that OH is essential to the metamictization process. Aines and Rossman (1985, 1986) hypothesize that OH actually stabilizes the metamict state of radiation-damaged zircon.

Not only is the role of H_2O in the metamictization process and its effect on the stability of metamict zircon open to question, but the identity of the hydrous species, whether H_2O or OH, is not well established. Thorite ($ThSiO_4$) is isostructural with zircon, but there is only limited solid solution with it. In thorite that has experienced relatively low α-decay event doses and is only partially metamict, Lumpkin and Chakoumakos (1988) have established that OH is present in the structure. At higher doses, sufficient to surpass the saturation dosage for total metamictization, they report that several weight percent H_2O coexists with the OH. Similar studies relating the hydrous species in zircon to the accumulated α-decay event dose have not been performed. These problems were the second impetus for our study and ultimately became its major focus.

Analytical techniques

The weighted mean radioactivity of each zircon was determined on crushed fractions in a scintillation counter (Silver and Deutsch, 1963). The α-activity resulting from decay of both U and Th is expressed in ppm eU, the equivalent U content (in secular equilibrium) necessary to produce the measured activity. The scintillation counter was repeatedly calibrated with homogeneous standard zircon from the Pacoima Canyon Pegmatite (Neuerburg, 1954; Silver et al., 1963) that had been analyzed by isotope dilution mass spectrometry for U and Th in several laboratories. The calibration was checked by independent isotope dilution analysis of several hundred zircon fractions measured with the counter. Three of the zircon specimens with low to intermediate radioactivity and one metamict zircon used in these experiments were analyzed independently by isotope dilution methods to establish both U and Th concentrations and to test the uniformity of the ages of the zircon population.

A Perkin-Elmer model 180 double-beam grating infrared spectrometer and a Nicolet 60SX FTIR were used to obtain IR spectra of the zircons. Transmission spectra in the range 2100–250 wavenumbers (cm^{-1}) were obtained on 1 mg fractions of the scintillation counter samples (finely ground, dispersed in pressed and dried 200-mg KBr pellets). Polarized and unpolarized transmission spectra in the range 4000–1300 cm^{-1} were obtained on polished, single-crystal zircon plates cut parallel to the c-axis. Plates 500–1000 μm thick were best for study of the weak absorption bands above 2000 cm^{-1}, including the O-H stretching region at around 3500 cm^{-1}. Plates 100–400 μm thick were required for the stronger absorption bands below 2000 cm^{-1}. Polarized reflection spectra in the range 4000–250 cm^{-1} were also obtained on a few polished plates.

A MAC-5 electron microprobe was used for chemical analyses of the polished, single-crystal zircon plates. Concentrations of 29 elements were determined, including major elements, U, Th, Pb, Y, and most of the REEs. The majority of standards used for the analyses were mineral samples or synthetic oxides—F and P, fluorapatite; Na, albite; Mg, periclase; Al and Ca, anorthite; Si, quartz; K, microcline; Ti, rutile; Mn, garnet; Fe, fayalite; Zr and Hf, zircon; Nb, synthetic NbO; Ta, synthetic $KTaO_3$; Pb, synthetic $PbCO_3$; Th, synthetic ThO_2; and U, synthetic UO_2. Standards for Y and the REEs were Ca-Al-silicate glasses, doped with approximately 4% of the rare earths, synthesized by Drake and Weill (1972). X-ray peaks for the minor and trace elements were chosen to avoid interference by those of the major elements as well as mutual overlaps. Backgrounds on each side of the measured peaks were chosen away from peaks of the other elements. $K\alpha$ lines of F, Na, Mg, and Al were measured using a KAP crystal. $K\alpha$ lines of Si, P, Ca, and Ti; $L\alpha$ lines of Y, Zr, and Nb; $M\alpha$ lines of Hf and Th; and the $M\beta$ line of Pb were measured using a PET crystal. $K\alpha$ lines of Fe and Mn; $L\alpha$ lines of La, Ce, Nd, Sm, Gd, Tb, Er, Yb, Lu, and Ta; $L\beta$ lines of Dy and Ho; and the $M\beta$ line of U were measured using an LiF crystal. Beam sizes of up to 25 μm were used in order to avoid damaging the more metamict samples. Probe data were reduced using Bence-Albee corrections.

X-ray powder diffraction patterns were obtained on zircon samples with an internal standard of spectroscopically pure rutile using a Norelco powder diffractometer. Patterns were obtained from 18 to 38° 2θ using Ni-filtered CuKα radiation at 40 kV and 20 mA. The positions of diffraction maxima were measured near the tops of the peaks rather than at their half-heights in order to avoid the problems caused by skewed peaks in radiation-damaged samples.

Sample characterization

The suite of zircon samples from Sri Lanka used in this study was chosen for four reasons: the samples have a wide range of U contents (Table 1); those analyzed have experienced less than 20% Pb loss, as shown by isotopic studies (Tilton et al., 1957; Pidgeon et al., 1966; Kröner et al., 1987); they have not been annealed, as shown by X-ray powder diffraction studies (Silver and Woodhead, in preparation); and most are large enough for a variety of optical and infrared spectroscopic studies. All of these samples were obtained originally from the U.S. National Museum, and many were used by Holland and Gottfried (1955). All but sample 6500 are from cut gemstones up to about ½ cm in diameter, generally free of fractures and inclusions. Sample 6500 is an uncut pebble about 1½ cm in diameter. It appears black in hand specimen, but reddish-brown when thin. The history of most of our samples prior to the time we acquired them is not known. Thus some of them may have been heated in an open

TABLE 1. Properties of Sri Lanka gem zircon samples

Zircon sample	Color	eU (ppm)	550 Ma α-dose × 10^{-15}	Probe analyses U* (ppm)	Probe analyses Hf/Zr ratio	Isotope dilution analyses U** (ppm)	Isotope dilution analyses Th** (ppm)	*a* (Å)	*c* (Å)	Unit-cell *V* (Å³)
2916A	straw	20	0.04	BAL†	0.015			ND‡	ND	ND
2916B	very pale straw	20	0.04	BAL	0.016	17.8(1)**	2.98(5)**	6.612(1)	5.994(1)	262.05
2916C	dark straw	20	0.04	BAL	0.013			ND	ND	ND
ZIN-1	straw	60	0.11	BAL	0.016			ND	ND	ND
106531A	straw	155	0.28	BAL	0.009			ND	ND	ND
3-2	dark straw	630	1.1	BAL	0.014	581(2)	137.7(5)	6.622(1)	6.034(1)	264.60
3-12	yellow	1020	1.8	BAL	0.020			6.646(1)	6.061(2)	267.71
3-11	straw yellow	1580	2.8	BAL	0.022			6.667(2)	6.095(5)	270.92
3-4	pale yellow	1600	2.9	1800 ± 860*	0.035			6.655(4)	6.073(2)	268.97
3-35	pale yellow	1935	3.5	2100 ± 1000	0.011			6.700(2)	6.121(1)	274.77
3-32	pale yellow	1940	3.5	ND	ND	1751(3)	126.4(5)	6.722(2)	6.123(3)	276.67
3-1	green-yellow	2025	3.7	2000 ± 490	0.022			6.694(9)	6.141(10)	275.18
1-42	green	4660	8.4	3000 ± 240	0.035			amorph	amorph	amorph
6500	very dark brown	6500	11.7	7600 ± 1700	0.059	5950(10)	ND	amorph	amorph	amorph
1-21	yellow-green	6725	12.1	7900 ± 1100	0.045			amorph	amorph	amorph
2-4	green	ND	(12.5)	6900 ± 330	0.044			amorph	amorph	amorph
1-30	green	7220	13.0	6400 ± 400	0.037			amorph	amorph	amorph
1-24	green	8290	14.9	6700 ± 450	0.063			amorph	amorph	amorph

* Electron microprobe analyses ±nnn is the range of analyses of different points resulting from zonation.
** Isotope dilution analysis; (*n*) denotes two standard deviations error of least unit cited.
† BAL = below analysis limit—too low for accurate electron microprobe analysis.
‡ ND = not determined.

fire, a common practice among zircon collectors in Sri Lanka. Sample 6500 did not undergo such heating.

Sri Lanka gem zircon samples are believed to be derived from late-stage pegmatites in the polymetamorphic Highland Group of metamorphic rocks (Munasinghe and Dissanayake, 1981; Kröner et al., 1987). They are not found in situ, but rather as rounded pebbles in stream deposits. However, because they plot on the same chord on a Concordia diagram (Silver and Woodhead, unpublished data) and have similarly low Th/U ratios, they appear to have related, if not identical, sources. We treat them here as a single suite as did Holland and Gottfried (1955).

RESULTS

The Sri Lanka zircon samples we studied have between 20 and 8290 ppm eU (Table 1). Based on the 550 Ma age of the Sri Lanka suite (Gottfried et al., 1956), their calculated total α-decay event dosage is between 0.05 and 14.7 × 10^{15} α-decay events per mg. Samples with eU below ~2000 ppm are yellow or straw colored while those with greater eU are green or brown.

Some of the zircon samples exhibit oscillatory zoning (Sommerauer, 1974; Sahama, 1981; Chakoumakos et al., 1987), evident from varying low-order birefringence colors on appropriately cut thick sections of high-eU samples (prepared for single-crystal transmission IR). Electron microprobe analyses of zoned samples show that lower birefringence correlates with higher U contents in each case. For samples with 1600 ppm eU or more, electron microprobe analyses supported the equivalent U contents determined by scintillation counter and indicated that variability of 20% or more between zones is common (Table 1). Th contents of all samples are <1000 ppm, the effective detection limit of the electron microprobe measurements, suggesting a Th/U weight ratio of <0.2 for the metamict samples. Hf/Zr atom ratios exhibit a wide range from 0.009 to 0.063 and have a positive correlation with eU such that Hf/Zr = 0.013 + 5 × 10^{-6} eU and r^2 = 0.83 (Fig. 1). No other substituents were statistically significant in the electron microprobe analyses. Isotope dilution analyses of four samples covering a wide range of degree of metamictization yield U and Th contents in close agreement with measured eU and Th/U weight ratios in the ~0.07–0.23 range.

X-ray powder diffraction patterns of a number of the samples show a systematic increase in unit-cell parameters with U content up to just over 2000 ppm eU (Fig. 2). X-ray diffraction maxima shifted to lower 2θ values, and became broader and markedly skewed (Holland and Gottfried, 1955; Murakami et al., 1986) in the partially metamict zircon samples. For those samples with greater U contents the unit-cell parameters could not be determined because they all do not give X-ray diffraction patterns and thus are metamict.

The IR spectrum of zircon is strongly affected by metamictization as can be seen in Figures 3 and 4 showing, respectively, powder absorption spectra between 1500 and 250 cm^{-1} and polarized single-crystal absorption spectra between 2000 and 1400 cm^{-1}, of three zircon samples with different U contents and different degrees of metamictization. Bands resulting from the fundamental vibration modes of zircon (Hubin and Tarte, 1971) occur in the region between 1000 and 300 cm^{-1} in Figure 3. The three strong, sharp bands at 433, 384, and 312 cm^{-1} in the crystalline zircon spectrum, representing external (lattice) vibration modes, are weakened by radiation damage in the partially metamict zircon spectrum and missing in

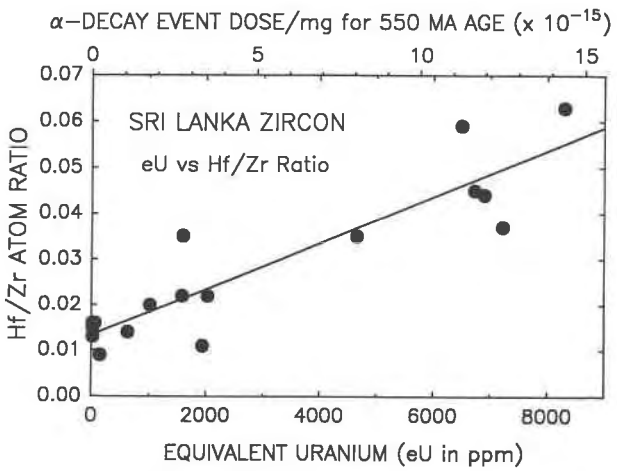

Fig. 1. Hf/Zr atom ratio for Sri Lanka gem zircon samples, measured by electron microprobe, as a function of equivalent U (eU) measured by scintillation counter. Calculated total α-decay event dosage based on a 550 Ma age for Sri Lanka gem zircon samples is shown across the top. The linear regression best fit to the data is shown; Hf/Zr = 0.013 + 5 × 10^{-6} eU, r^2 = 0.83.

that of the totally metamict sample. The bands at 973 and 892 cm^{-1} representing internal stretching modes of the $[SiO_4]^{4-}$ anion (Dawson et al., 1971; Adams, 1973), and at 611 cm^{-1}, an internal bending mode of the $[SiO_4]^{4-}$ anion, are progressively broadened and weakened with metamictization (Deliens et al., 1977).

Plots of the behavior of some of the fundamental-mode bands as functions of eU and calculated total α-decay event dosage are shown in Figure 5. The intensities of the external-mode bands at ~384 and ~312 cm^{-1} decrease dramatically with equivalent U up to 2000 ppm eU and are negligible beyond that point (Fig. 5 top). The disappearance of the external-mode bands coincides with the eU content beyond which the samples exhibit no X-ray diffraction patterns and is thus another indicator of total

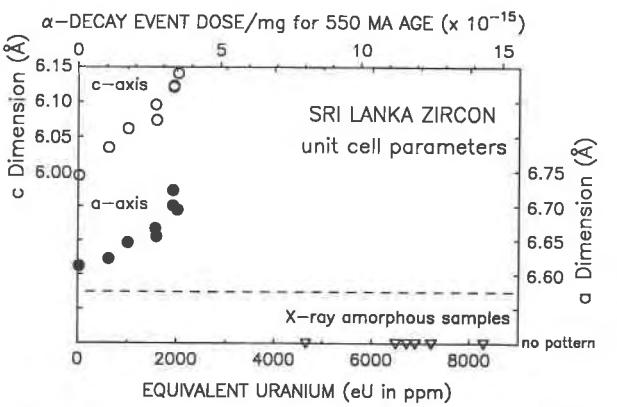

Fig. 2. Unit-cell parameters measured by powder X-ray diffraction as a function of eU and α-decay event dosage. Only samples with less than approximately 2500 ppm eU yielded diffraction patterns; those with more did not diffract X-radiation.

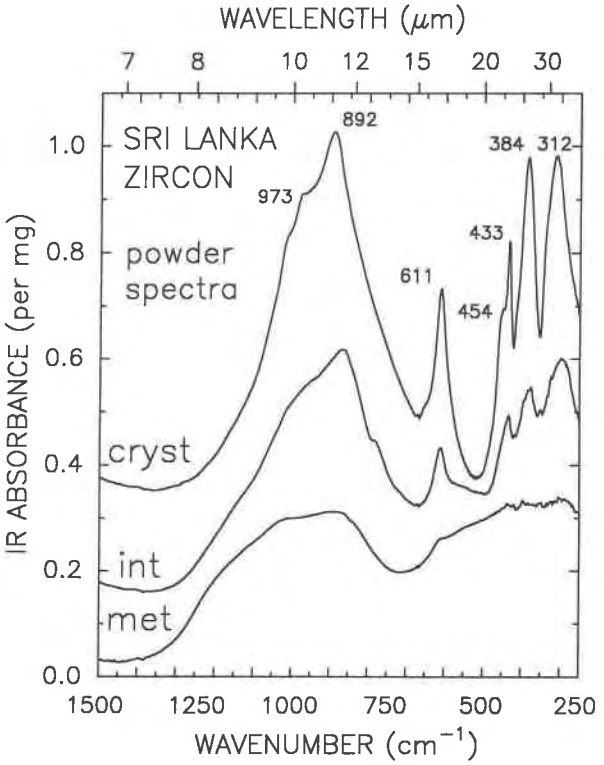

Fig. 3. IR powder spectra in the range 1500–250 cm^{-1} of three Sri Lanka gem zircon samples given in units of absorbance per mg as a function of wavenumber; cryst = Sri Lanka gem zircon 2916C, nonmetamict, 20 ppm eU. Absorption bands representing internal $[SiO_4]^{4-}$ stretching modes are at 973 and 892 cm^{-1}. Those for internal $[SiO_4]^{4-}$ bending modes are at 611 and 454 cm^{-1}. The band at 433 cm^{-1} represents external rotational vibration of the essentially rigid $[SiO_4]^{4-}$ tetrahedron; those at 384 and 312 cm^{-1} represent external translational vibrations; int = Sri Lanka gem zircon 3-11, partially metamict, 1580 ppm eU. Note the general loss of intensity of all IR absorption bands resulting from radiation damage; met = Sri Lanka zircon 6500, metamict, 6500 ppm eU. Bands representing external modes are nearly absent. Those of internal vibration modes have weakened and broadened.

metamictization. The intensities of the internal-mode band at ~892 cm^{-1} are more scattered but decrease with eU up to 2000 ppm (Fig. 5 bottom). Beyond that value they remain easily detectable at 10–20% of their intensities in the least radiation-damaged samples.

According to Dawson et al. (1971), the bands in the 2000 to 1400 cm^{-1} region shown in Figure 4 result from two-phonon combination modes involving stretching and bending modes of the $[SiO_4]^{4-}$ anion. They become weaker and broader with metamictization while the relatively transparent window at 1650–1700 cm^{-1} becomes more opaque, corroborating the work of Wasilewski et al. (1973), who showed that absorption at 1666 cm^{-1} increases with degree of metamictization.

A more striking effect of metamictization is the destruction of anisotropy. In crystalline zircon, absorption

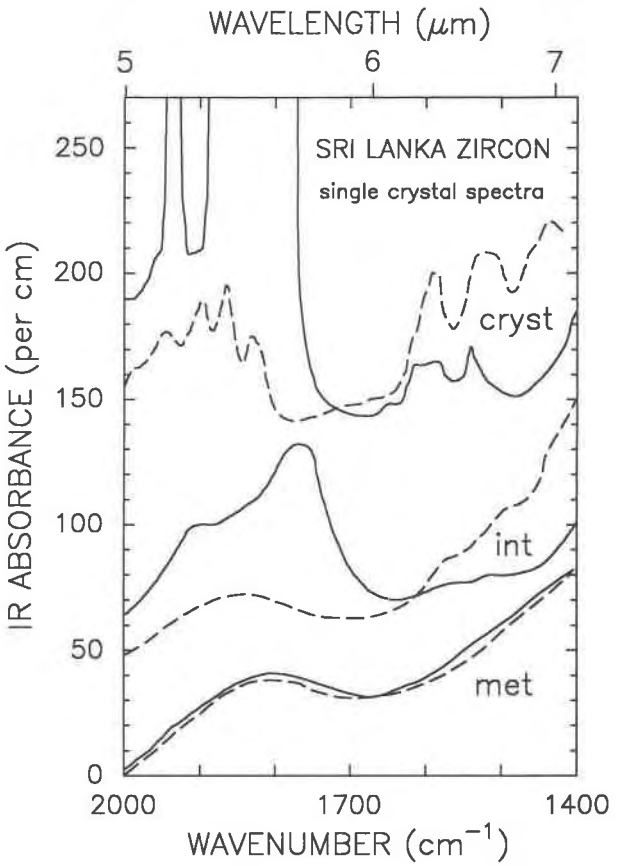

Fig. 4. Polarized single-crystal IR absorption spectra of three Sri Lanka gem zircon samples cut parallel to the c-axis in the range 2000–1400 cm^{-1} given as absorbance per cm as a function of wavenumber. The solid line shows the spectrum for which **E** // **c**; the dashed line shows the spectrum for which **E** ⊥ **c**; cryst = Sri Lanka gem zircon 2916C, nonmetamict, 20 ppm eU. The strong, sharp bands result from combination modes involving internal stretching and bending modes of the $[SiO_4]^{4-}$ tetrahedron. The IR absorption pattern is markedly anisotropic. Absorption at ~1780 cm^{-1} for **E** ⊥ **c** is very low compared to that for the spectrum with **E** // **c** at ~1780 cm^{-1}. Absorption in the 1650–1700 cm^{-1} range is low for both polarization conditions; int = Sri Lanka gem zircon 3-35, partially metamict, 1935 ppm eU. The IR bands are broader and less anisotropic, resulting in an increase in absorption at 1650–1700 cm^{-1}; met = Sri Lanka zircon 6500, metamict, 6500 ppm eU. The IR absorption pattern is essentially isotropic; absorption at 1650–1700 cm^{-1} is high.

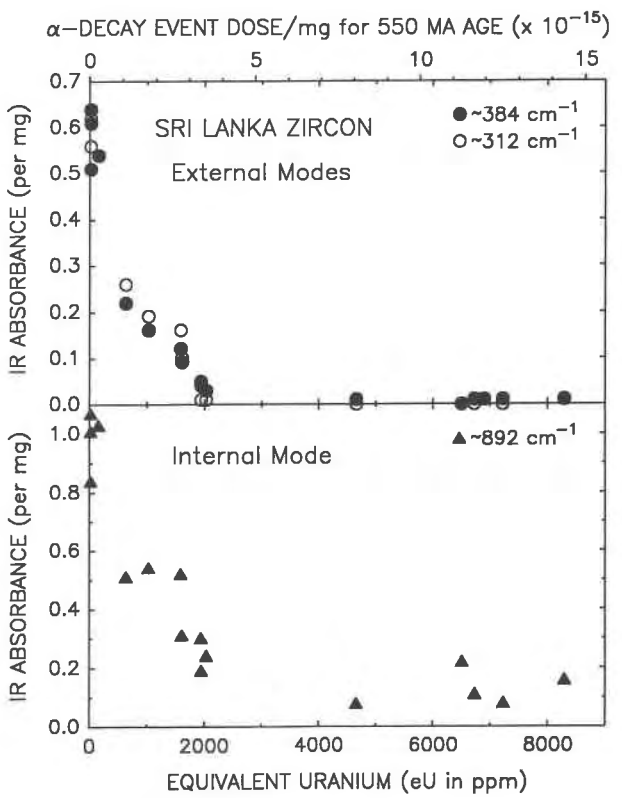

Fig. 5. IR absorption band intensities, given as absorbance per mg, as functions of eU and α-decay event dosage. **(top)** Intensity of external $[SiO_4]$ translation mode bands at ~384 and ~312 cm^{-1}. Band intensity decreases with increasing U content up to approximately 2500 ppm eU and is negligible above that value. **(bottom)** Intensity of internal $[SiO_4]^{4-}$ stretching-mode band at ~892 cm^{-1}. Band intensity decreases with increasing U content up to approximately 2500 ppm eU but does not decrease to zero at higher eU levels.

at ~1780 cm^{-1} is much weaker when the electric vector is oriented perpendicular to the c-axis than when parallel to it. The absorption ratio between the two polarization directions is a function of eU for partially metamict zircon samples up to approximately 2500 ppm eU (Fig. 6). It is 1.0 beyond that point, indicating that the metamict samples are all isotropic with respect to IR radiation.

Figure 7 shows polarized single-crystal absorption spectra between 4000 and 2000 cm^{-1} for the same three zircon samples as in Figure 4. The weak band at ~2740 cm^{-1} in the spectrum for which **E** // **c** of the crystalline zircon represents a three-phonon combination mode (Dawson et al., 1971). Those at ~3095 and ~3185 cm^{-1} in the spectrum for which **E** ⊥ **c** apparently also result from three-phonon combination modes. The strength of the band at ~2740 cm^{-1} in the orientation for which **E** // **c** decreases with eU for partially metamict zircon and is zero for totally metamict grains as shown in Figure 8.

The broad isotropic band at about 3500 cm^{-1} in the metamict zircon (Fig. 7) indicates the presence of a hydrous species, either OH or H_2O, and results from the O-H stretching mode. Although O-H stretching bands are usually broader for H_2O than OH in minerals, often appearing much like the band in the metamict zircon spectrum, the only certain way to distinguish H_2O from OH is by the presence of the H-O-H bending-mode band at about 1600 cm^{-1} or the combination mode involving H_2O at approximately 5200 cm^{-1}. The molar absorption coefficients of the IR bands of H_2O or OH are not known in

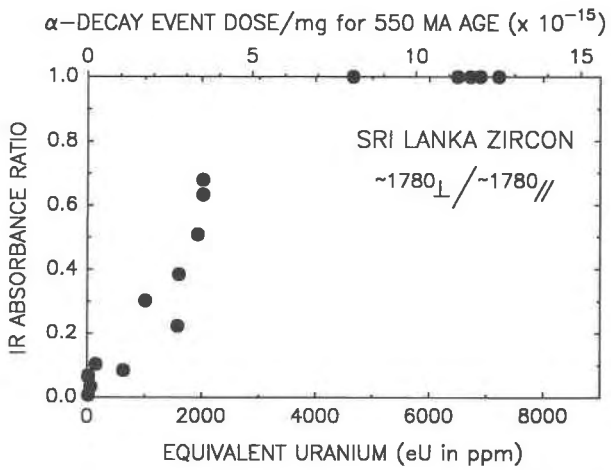

Fig. 6. IR absorbance ratio (**E** ⊥ **c**) /(**E** // **c**) at ~1780 cm^{-1} as a function of eU and α-decay event dosage. The ratio increases with U content up to approximately 2500 ppm eU, beyond which value the samples are no longer anisotropic.

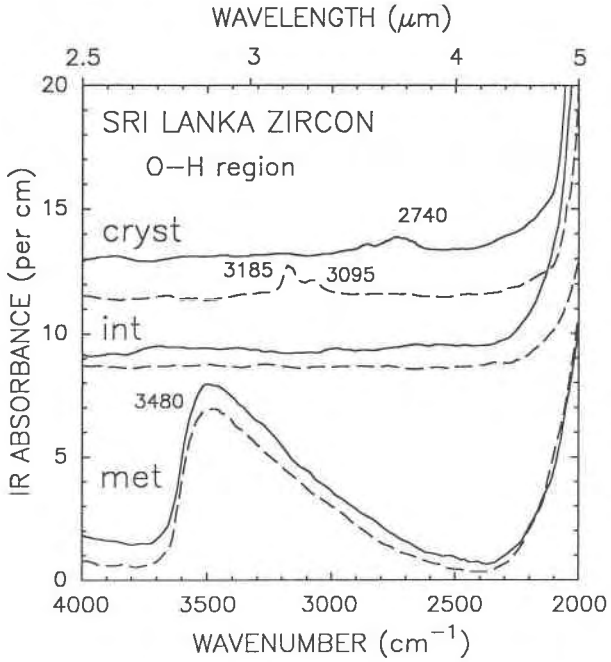

Fig. 7. Polarized single-crystal IR absorption spectra of three Sri Lanka gem zircons cut parallel to the c-axis in the range 4000–2000 cm^{-1} given in units of absorbance per cm as a function of wavenumber. The solid line shows the spectrum for which **E** // **c**; the dashed line shows the spectrum for which **E** ⊥ **c**; cryst = Sri Lanka gem zircon 2916C, nonmetamict, 20 ppm eU. The IR absorption pattern is anisotropic. The bands at ~2740 cm^{-1}, **E** // **c**, and at ~3095 and ~3185 cm^{-1}, **E** ⊥ **c**, are three-phonon combination modes of $[SiO_4]^{4-}$ internal vibrations. The sample is free of OH or H_2O as indicated by the absence of a band in the O-H stretching region around 3500 cm^{-1}; int = Sri Lanka gem zircon 3-35, partially metamict, 1935 ppm eU. The band at ~2740 cm^{-1} is too weak to be seen at this scale, but the sample is not isotropic. There is no OH or H_2O present; met = Sri Lanka zircon 6500, metamict, 6500 ppm eU. The IR absorption pattern is essentially isotropic. The strong band at ~3500 cm^{-1} represents the O-H stretching mode and results from the presence of OH in the sample.

either crystalline or metamict zircon but those of the H_2O bands are probably within the range of those determined for liquid H_2O and silicate glasses (Rossman, 1988; Newman et al., 1986). The bending-mode band at ~1600 cm^{-1} can be expected to be approximately 2–4 times weaker than the stretching-mode band, and the combination mode band at ~5200 cm^{-1} can be expected to be approximately 30–70 times weaker. Thus if the hydrous species in the metamict sample 6500 shown in Figure 7 were entirely H_2O the strength of H_2O bands at ~1600 and ~5200 cm^{-1} would be at least 1.5 and 0.1 absorbance units per cm, respectively.

There is no indication of the fundamental H-O-H bending-mode band in any of the hydrous samples, indicating that the hydrous species present is predominantly OH rather than H_2O. As can be seen in Figure 4, however, zircon is rather opaque at 1600 cm^{-1} and its IR spectrum varies strongly with degree of metamictization. Thus it is possible that in metamict zircon H_2O might not be unambiguously distinguishable from OH at very low H_2O concentrations.

The zircon spectrum is rather flat around 5000 cm^{-1}. In that region the band detection limit is approximately 0.02 absorbance units per cm on our spectrometer. An H_2O content that produced a stretching-mode band of 7 absorbance units per cm (as in sample 6500 shown in Fig. 7) would be easily detectable. There is no indication of the combination mode band at about 5200 cm^{-1} in any spectrum. The absence in the same spectrum of both H_2O bands indicates that at least 80% of the hydrous component in the Sri Lanka gem zircon samples is OH.

The calibration relating IR absorption intensity in the OH region to OH content in zircon is not established. The amount of OH can be estimated, however, from published IR molar absorptivity data for the broad OH-stretching band in glass (Newman et al., 1986) and H_2O (Thompson, 1965). Using a simple Beer's law calculation, the hydrous component in our zircon with the strongest O-H stretching bands, sample 6500, is on the order of 0.02–0.04 wt% (expressed as H_2O).

The OH content of the Sri Lanka gem zircon samples is related to metamictization in an interesting way. Nearly all the samples with eU below 2500 ppm contain no OH or H_2O (Fig. 9), while all those with higher U contents contain OH. There is no correlation between OH content and U (or Hf) content in the metamict grains, however. The two zircon samples with <2500 ppm eU that contain detectable OH are both zoned. Electron microprobe analyses of sample 3-1, with an eU content just below the amount sufficient to cause total metamictization, indicate considerable variability in U content and suggest that the OH detected may be predominantly in metamict zones or at the boundary between zones. In-

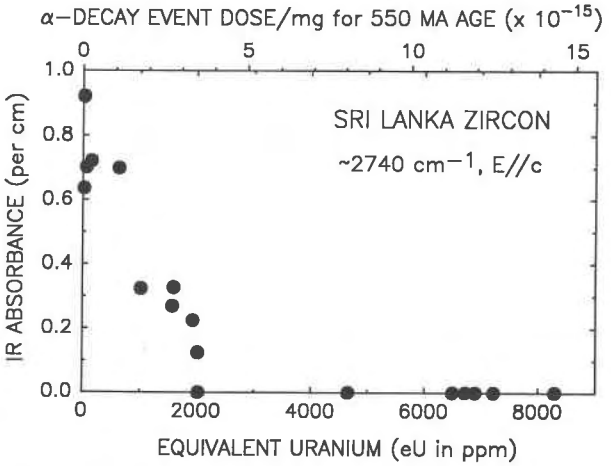

Fig. 8. IR absorbance for polarized single crystal spectra (**E // c**), given in units of absorbance per cm at ~2740 cm^{-1}, as a function of eU and α-decay event dosage. Band intensity decreases with increasing U content up to about 2500 ppm eU and is negligible above that value.

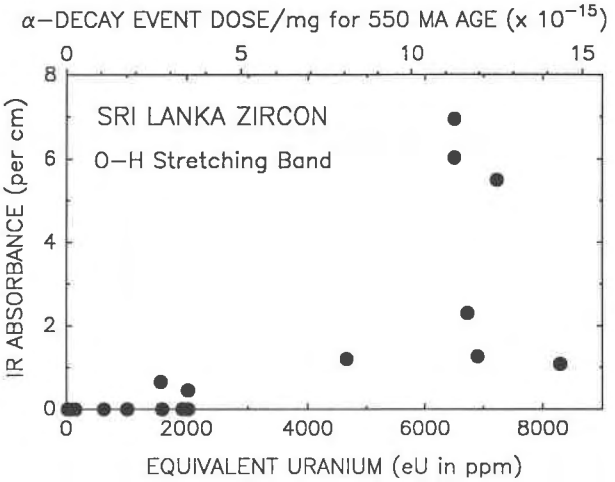

Fig. 9. IR absorbance in the O-H stretching region at about 3500 cm^{-1} for unpolarized single crystal spectra, given in units of absorbance per cm, as a function of eU and α-decay event dosage. All samples that are not completely metamict contain little or no OH or H_2O. Although metamict samples all contain detectable OH, there is no relation between OH content and U content.

deed, a second sample of the same grain showed no OH. Electron microprobe analyses also indirectly suggest the existence of high-U zones in sample 3-11. The two analyzed points gave values <1000 ppm eU, considerably less than the average content of 1580 ppm eU. Zones enriched in U to a similar degree probably exist and may be the sites of the OH detected. It thus appears that for zircon near the transition point, OH is present if U zonation is sufficient to produce metamict zones in otherwise partially metamict grains.

Discussion

Infrared methods provide several indicators of metamictization to complement X-ray diffraction and optical techniques. These include loss of the external-mode bands at 433, 384, and 312 cm^{-1}, loss of the combination-mode band at 2740 cm^{-1}, and isotropism of single-crystal absorption patterns. These indicators consistently show that, among the Sri Lanka gem zircon samples studied, only those with >2500 ppm eU are entirely metamict. The calculated dosage level at which 550 Ma Sri Lanka gem zircon samples become metamict is between 3.7×10^{15} α-decay events/mg (sample 3-1, 2025 ppm eU) and 8.5×10^{15} α-decay events/mg (sample 1-42, 4660 ppm eU). The slopes of the IR data (Figs. 5, 6, and 8) imply that the total metamictization occurs at about 2500 ppm eU, a calculated dosage of 4.5×10^{15} α-decay events/mg for these zircon samples. That is the same value at which Holland and Gottfried (1955) found that unit-cell parameters no longer increase with dosage, but is well below the dosage of 1×10^{16} α-decay events/mg at which they found no trace of X-ray diffraction lines. Headley et al. (1982) found that a calculated dosage of 1×10^{16} α-decay events/mg caused the loss of electron diffraction patterns for a zircon specimen from Saudi Arabia. Murakami et al. (1986) found that Sri Lanka zircon samples with over 8×10^{15} α-decay events/mg exhibited no X-ray diffraction patterns. Given the observed variability in U content for Sri Lanka zircon, the higher dosage level required for complete metamictization noted by others may simply be a result of the existence of zones or domains with lower than average U contents. It may also be the result of small degrees of annealing as proposed by Holland and Gottfried (1955) and supported by Weber and Maupin (1988) in their study of the behavior of ^{238}Pu-doped synthetic zircon, which no longer gave X-ray diffraction at a dosage of 6.78×10^{15} α-decay events/mg.

Changes in the IR spectrum of zircon with metamictization give some insight into the structure of the metamict state. The external-mode bands (which to a first approximation involve only Zr-O bonds) are missing in metamict samples, indicating that the immediate environment of the Zr^{4+} ion must be highly disturbed—with sufficient variation in Zr-O bond distances and Zr-O-Si bond angles to destroy the acoustic modes present in crystalline zircon. This is consistent with the conclusions of Nakai et al. (1987) based on EXAFS analyses and those of Farges and Calas (1991) based on both EXAFS and XANES analyses. In contrast, the internal-mode bands (which to a first approximation involve only Si-O bonds) are preserved, albeit weakened and broadened, indicating that the immediate environment of the Si^{4+} ion (the $[SiO_4]^{4-}$ tetrahedron) must be essentially retained. This is consistent with the conclusions of Sugiyama and Waseda (1989) as derived by X-ray scattering radial distribution function studies. The broadening of the fundamental- and

combination-mode bands involving internal $[SiO_4]^{4-}$ vibrations indicates that the D_{2d} symmetry of the $[SiO_4]^{4-}$ tetrahedron is lost and that the average local environment of the silica tetrahedron becomes progressively less ordered up to the occurrence of total metamictization; this probably results from rotation and tilting of the $[SiO_4]^{4-}$ tetrahedron in response to displacements of Zr. This is consistent with the data of Farges and Calas (1991). The intensities of the internal-mode bands are approximately constant (Fig. 5 bottom) beyond that point, however, suggesting that the local environments do not continue to change dramatically with higher dosage rates in samples that are already metamict.

For the most part, OH is present only in metamict or nearly metamict samples. Within this group of samples there is no obvious relationship between OH content and eU, suggesting that Sri Lanka gem zircon samples initially crystallized without OH, and OH was incorporated only after radiation damage passed some threshold level—apparently the point of total metamictization for most grains. Because the amount of OH incorporated in our zircon samples does not correlate with U content, it is likely that factors such as f_{H_2O}, temperature, and the period of time subsequent to metamictization were important factors in incorporation of OH. Zircon with higher eU contents becomes metamict faster and thus may interact with fluids for longer times subsequent to metamictization. For example, zircon 1-24, with 8290 ppm eU, must have become metamict at about 400 Ma; whereas zircon 1-42, with 4660 ppm eU, did not become metamict until about 250 Ma, thus raising the possibility that their interaction with H_2O in the geological environment has been different.

Our data show that zircon with no OH spans virtually the entire range from crystalline to metamict; OH cannot be necessary to the metamictization process, as concluded by Caruba et al. (1985). In short, H_2O and OH are not important participants in the metamictization process but may be merely fortuitous fellow travelers. They may still have an important role in postmetamictization stability, but that role needs to be further evaluated in light of our results.

Conclusions

IR spectra of zircon depend strongly on the degree of metamictization. Radiation damage causes the intensity of both fundamental- and combination-mode bands to decrease drastically. The ultimate result is the loss of the bands representing vibration modes involving Zr-O bonds. Consequently, the structure of metamict zircon must consist of distorted and disoriented, isolated silica tetrahedra with few if any undisplaced Zr cations.

IR indicators of metamictization (approach to isotropy and the loss of external vibration-mode bands) and X-ray diffraction results both yield a total dosage of about 4.5 $\times$ 10^{15} α-decay events/mg as being necessary for complete metamictization. Samples with greater accumulated dosages do not yield X-ray diffraction patterns and are isotropic to both visible and infrared radiation. Variability in U content or subsequent annealing may yield partially metamict domains in otherwise metamict samples.

The only hydrous species detectable in the Sri Lanka gem zircon samples studied is OH. The absence of OH in most samples that are less than fully metamict indicates that OH is not at all necessary to the metamictization process. The OH appears to be absorbed by zircon that initially has no OH only after radiation damage has altered its structure sufficiently—apparently something that occurs only when zircon is metamict or nearly so. The effect of hydrous species on the ultimate stability of the metamict state is not known.

Acknowledgments

This research was funded in part by National Science Foundation grants EAR-7919987, 8618200, and 8916064. We thank David Gottfried, Heinrich Holland, and Frank Senftle (USGS, Reston, Virginia) for samples included in this work. We thank Rodney Ewing, François Farges, and John Hughes for their helpful comments on the manuscript. This study is Caltech contribution no. 4606.

References cited

Adams, D.M. (1973) A descriptive introduction to analysis of the vibrational spectra of solids. Coordination Chemistry Reviews, 10, 183–193.

Aines, R.D., and Rossman, G.R. (1985) The high temperature behavior of trace hydrous components in silicate minerals. American Mineralogist, 70, 1169–1179.

——— (1986) Relationships between radiation damage and trace water in zircon, quartz, and topaz. American Mineralogist, 71, 1186–1193.

Bursill, L.A., and MacLaren, A.C. (1966) Transmission electron microscope study of natural radiation damage in zircon ($ZrSiO_4$). Physica Status Solidi, 13, 331–343.

Caruba, R., Baumer, A., Ganteaume, M., and Iacconi, P. (1985) An experimental study of hydroxyl groups and water in synthetic and natural zircons: A model of the metamict state. American Mineralogist, 70, 1224–1231.

Chakoumakos, B.C., Murakami, T., Lumpkin, G.R., and Ewing, R.C. (1987) Alpha-decay-induced fracturing in zircon: The transition from the crystalline to the metamict state. Science, 236, 1493, 1497, 1556–1559.

Dawson, P., Hargreave, M.M., and Wilkinson, G.R. (1971) The vibrational spectrum of zircon ($ZrSiO_4$). Journal of Physics C: Solid State Physics, 4, 240–256.

Deliens, M., Delhal, J., and Tarte, P. (1977) Metamictization and U-Pb systematics—A study by infrared absorption spectrometry of Precambrian zircons. Earth and Planetary Science Letters, 33, 331–344.

Drake, M.J., and Weill, D.F. (1972) New rare earth element standards for electron microprobe analysis. Chemical Geology, 10, 179–181.

Farges, F., and Calas, G. (1991) Structural analysis of radiation damage in zircon and thorite: An X-ray absorption spectroscopic study. American Mineralogist, 76, 60–73.

Frondel, C., and Collette, R.L. (1957) Hydrothermal synthesis of zircon, thorite and huttonite. American Mineralogist, 42, 759–765.

Gottfried, D., Senftle, F.E., and Waring, C.L. (1956) Age determination of zircon crystals from Ceylon. American Mineralogist, 41, 157–161.

Headley, T.J., Ewing, R.C., and Haaker, R.F. (1982) TEM study of the metamict state. Physics of Minerals and Ore Microscopy, Proceedings of the 13th general meeting of the International Mineralogical Association at Varna, Bulgaria, September 19–25, 281–289.

Holland, H.D., and Gottfried, D. (1955) The effect of nuclear radiation on the structure of zircon. Acta Crystallographica, 8, 291–300.

Hubin, R., and Tarte, P. (1971) Étude infrarouge des orthosilicates et des

orthogermanates—IV. Structures scheellite et zircon. Spectrochimica Acta, 27A, 683–690.

Kröner, A., Williams, I.S., Compston, W., Baur, N., Vitanage, P.W., and Perrera, L.R.K. (1987) Zircon ion microprobe dating of high-grade rocks in Sri Lanka. Journal of Geology, 95, 775–791.

Lumpkin, G.R., and Chakoumakos, B.C. (1988) Chemistry and radiation effects of thorite-group minerals from the Harding pegmatite, Taos County, New Mexico. American Mineralogist, 73, 1405–1419.

Munasinghe, T., and Dissanayake, C.B. (1981) The origin of gem stones of Sri Lanka. Economic Geology, 76, 1216–1225.

Murakami, T., Chakoumakos, B.C., and Ewing, R.C. (1986) X-ray powder diffraction analysis of alpha-event radiation damage in zircon ($ZrSiO_4$). In D.E. Clark, W.B. White, and J. Machiels, Eds., Advances in ceramics, nuclear waste management II, p. 745–753. American Ceramic Society, Columbus, Ohio.

Nakai, I., Akimoto, J., Imafuku, M., Miyawaki, R., Sugitani, Y., and Koto, K. (1987) Characterization of the amorphous state in metamict silicates and niobates by EXAFS and XANES analyses. Physics and Chemistry of Minerals, 15, 113–124.

Neuerburg, G.J. (1954) Allanite pegmatite, San Gabriel Mountains, Los Angeles County, California. American Mineralogist, 39, 831–834.

Newman, S., Stolper, E.M., and Epstein, S. (1986) Measurement of water in rhyolitic glasses: Calibration of an infrared spectroscopic technique. American Mineralogist, 71, 1527–1541.

Pavlovic, S., and Krstanovic, I. (1965) Sur les possibilités de determination d'age absolu d'après les mesures cristallographiques du zircon. Colloque International de Géochronologie Absolue. Nancy, 3–8 Mai 1965. Sciences de la Terre, 10, 285–290.

Pellas, P. (1965) Étude sur la recristallisation thermique des zircons métamictes. Mémoires du Museum National d'Histoire Naturelle, Série C, Sciences de la Terre, 12, 227–253.

Pidgeon, R.T., O'Neill, J., and Silver, L.T. (1966) Uranium and lead isotopic stability in a metamict zircon under experimental hydrothermal conditions. Science, 154, 1538–1540.

——— (1973) Observations on the crystallinity and the U-Pb isotopic system of a metamict Ceylon zircon under experimental hydrothermal conditions. Fortschritte der Mineralogie, 50, 118.

Robinson, K., Gibbs, G.V., and Ribbe, P.H. (1971) The structure of zircon: A comparison with garnet. American Mineralogist, 56, 782–790.

Rossman, G.R. (1988) Vibrational spectroscopy of hydrous components. In Mineralogical Society of America Reviews in Mineralogy, 18, 193–206.

Sahama, T. (1981) Growth structure in Ceylon zircon. Bulletin de Minéralogie, 104, 89–94.

Silver, L.T. (1964) The relation between radioactivity and discordance in zircons. Nuclear Geophysics, National Academy of Sciences—National Research Council Publication 1075, 34–39.

Silver, L.T., and Deutsch, S. (1963) Uranium-lead isotopic variations in zircons: A case study. Journal of Geology, 71, 721–758.

Silver, L.T., McKinney, C.R., Deutsch, S., and Bollinger, J. (1963) Precambrian determinations in the western San Gabriel Mountains, California. Journal of Geology, 71, 196–214.

Sommerauer, J. (1974) Trace element distribution patterns and the mineralogical stability of zircon—An application for combined electron microprobe techniques. Electron Microscopy Society of Southern Africa, Proceedings, 4, 71–72.

——— (1976) Die chemisch-physikalische Stabilität natürlicher Zirkone und ihr U-(Th)-Pb System. Ph.D. dissertation. Eidgenössischen Technische Hochschule, Zürich.

Sugiyama, K., and Waseda, Y. (1989) Structural study of the metamict states by X-ray diffraction: In the case of naegite. Mineralogical Journal, 14, 303–309.

Thompson, W.K. (1965) Infrared spectroscopic studies of aqueous systems, I. Transactions of the Faraday Society, 61, 1635–1640.

Tilton, G.R., Davis, G.L., Wetherill, G.W., and Aldrich, T.L. (1957) Isotopic ages from granites and pegmatites. American Geophysical Union Transactions, 38, 360–371.

Vance, E.R. (1975) Alpha recoil damage in zircon. Radiation Effects, 24, 1–6.

Wasilewski, P.J., Senftle, F.E., and Vaz, J.E. (1973) A study of the natural α-recoil damage in zircon by infrared spectra. Radiation Effects, 17, 191–199.

Weber, W.J., and Maupin, G.D. (1988) Simulation of radiation damage in zircon. Nuclear Instruments and Methods in Physics Research, B32, 512–515.

Yada, K., Tanji, T., and Sunagawa, I. (1981) Application of lattice imagery to radiation damage investigation in natural zircon. Physics and Chemistry of Minerals, 7, 47–52.

——— (1987) Radiation induced lattice defects in natural zircon ($ZrSiO_4$) observed at atomic resolution. Physics and Chemistry of Minerals, 14, 197–204.

Manuscript received May 21, 1990
Manuscript accepted November 14, 1990